# Photochemistry of Nitric Oxide Adducts of Water-Soluble Iron(III) Porphyrin and Ferrihemoproteins Studied by Nanosecond Laser Photolysis

**Mikio Hoshino,*,† Koji Ozawa,† Hiroshi Seki,† and Peter C. Ford‡**

*Contribution from The Institute of Physical and Chemical Research, Wako, Saitama 351-01, Japan, and the Department of Chemistry, University of California, Santa Barbara, California 93106*

*Received April 23, 1993®*

**Abstract:** Water-soluble iron(III) porphyrin and ferrihemoproteins (methemoglobin, metmyoglobin, oxidized cytochrome *c*, and catalase) associate with NO to yield the nitric oxide adducts. The equilibrium constants for association of ferrihemoproteins and NO are 1 order of magnitude larger than that of the water-soluble iron(III) porphyrin which is free from protein, suggesting that the proteins offset the forward and backward reaction rates in the equilibrium reactions. Nanosecond laser photolysis studies of the nitric oxide adducts of metmyoglobin, oxidized cytochrome *c*, and catalase, (NO)$Mb^{III}$, (NO)$Cyt^{III}$, and (NO)$Cat^{III}$, have been carried out. The transient detected after laser flash photolysis of (NO)$Cat^{III}$ is identified as $Cat^{III}$. However, the transients observed for (NO)$Mb^{III}$ and (NO)$Cyt^{III}$ at 50 ns after laser pulsing are ascribed to $Mb^{III}_{tr}$ and $Cyt^{III}_{tr}$, respectively, with the absorption spectra different from those of uncomplexed $Mb^{III}$ and $Cyt^{III}$. In particular, the absorption spectrum of $Cyt^{III}_{tr}$ markedly differs from that of the uncomplexed $Cyt^{III}$. The species $Mb^{III}_{tr}$ and $Cyt^{III}_{tr}$ are found to change to $Mb^{III}$ and $Cyt^{III}$, respectively, within a few microseconds. The quantum yields for the photodissociation of NO from nitric oxide adducts of ferrihemoproteins are 1 order of magnitude less than that from the NO adduct of the water-soluble iron(III) porphyrin, probably due to fast geminate recombination reaction of NO and ferrihemoprotein in a heme pocket. The photochemistry of the nitric oxide adducts of hemoproteins and water-soluble iron(II) porphyrin is also described on the basis of laser phosolysis studies.

## Introduction

Iron(II) and iron(III) porphyrins, $Fe^{II}P$ and $Fe^{III}P$, interact with nitric oxide, NO, to yield the adducts (NO)$Fe^{II}P$ and (NO)$Fe^{III}P$.[1-3] It has been established by ESR experiments that (NO)$Fe^{II}P$ and (NO)$Fe^{III}P$ are respectively paramagnetic and diamagnetic: the spin state of the former is $S = {}^1/_2$ and the latter $S = 0$.[1-6] Recently, nitric oxide has been recognized to have important bioregulatory roles as the endothelium-derived relaxing factor in blood vessels, in the cytotoxic action of macrophages, and in neuronal communication in the brain.[7-11] Nitric oxide is known to be synthesized in vivo from L-arginine by the enzyme NO synthase.[12,13] Because NO is highly reactive toward both iron(II) and iron(III) porphyrins, it is expected that NO reacts in vivo with both ferric and ferrous forms of hemoproteins, giving rise to the formation of their nitrosyl adducts. Thus, quantitative studies on the interaction between NO and natural iron porphyrins assume increased importance.

The photochemistry of the $O_2$ adducts of hemoglobin and myoglobin has been extensively investigated by nanosecond and picosecond laser flash photolysis in order to elucidate the nature of the $Fe^{II}$–$O_2$ bond as well as the role of proteins in photodissociation of $O_2$ from the $O_2$ adducts.[14-19] The CO and NO adducts of both hemoproteins and synthetic iron(II) porphyrins have also been subjected to the laser photolysis studies.[20-37] However,

† The Institute of Physical and Chemical Research.
‡ University of California.
® Abstract published in *Advance ACS Abstracts*, September 15, 1993.

(1) Yonetani, T.; Yamamoto, H. In *Oxidases and Related Redox Systems*; King, T. E., Mason, S., Morrison, M., Eds.; University Park Press: Baltimore, MD, 1973; Vol. I, pp 278–298.
(2) Palmer, G. In *The Porphyrins*; Dolphin, D., Ed.; Academic Press: New York, 1979; Vol. IV, Part B, Chapter 6.
(3) Keilin, D.; Hartree, E. F. *Nature* **1973**, *139*, 548.
(4) Kon, H. *J. Biol. Chem.* **1968**, *243*, 4350–4357.
(5) Kon, H. *Biochem. Biophys. Res. Commun.* **1969**, *35*, 423–427.
(6) Kon, H. *Biochim. Biophys. Acta* **1975**, *379*, 105–113.
(7) Hibbs, J. B., Jr.; Vavrin, Z.; Taintor, R. R. *J. Immunol.* **1987**, *138*, 550–565.
(8) Liew, F. Y.; Cox, F. E. G. *Immunol. Today* **1991**, *17*, A17–A21.
(9) Bredt, D. S.; Hwang, P. M.; Glatt, C. E.; Lowenstein, C.; Reed, R. R.; Snyder, S. H. *Nature* **1991**, *351*, 714–718.
(10) Rad, R.; Beckman, J. S.; Bush, K. M.; Freeman, B. A. *J. Biol. Chem.* **1991**, *266*, 4244–4250.
(11) Lancaster, J. R., Jr.; Hibbs, J. B., Jr. *Proc. Natl. Acad. Sci. U.S.A.* **1990**, *87*, 1223–1227.
(12) Tayeh, M. A.; Marletta, M. A. *J. Biol. Chem.* **1989**, *264*, 19654–19658.
(13) Hibbs, J. B., Jr.; Taintor, R. R.; Vavrin, Z. *Science* **1987**, *235*, 473–476.
(14) Greene, B. I.; Hochstrasser, R. M.; Weisman, R. B.; Eaton, W. A. *Proc. Natl. Acad. Sci. U.S.A.* **1978**, *75*, 5255–5259.
(15) Chernoff, D. A.; Hochstrasser, R. M.; Steele, A. W. *Proc. Natl. Acad. Sci. U.S.A.* **1980**, *77*, 5606–5610.
(16) Saffran, W. A.; Gibson, Q. H. *J. Biol. Chem* **1977**, *252*, 7955–7958.
(17) Austin, R. H.; Beeson, K. W.; Eisenstein, L.; Fraunfelder, H.; Gunsalus, I. C. *Biochemistry* **1975**, *14*, 5355–5373.
(18) Petrich, J. W.; Poyart, C.; Martin, J. L. *Biochemistry* **1988**, *27*, 4049–4060.
(19) Valat, P.; Tourbez, H.; Alpert, B. *Laser Chem.* **1982**, *1*, 45–57.
(20) Cornelius, P. A.; Hochstrasser, R. M.; Steele, A. W. *J. Mol. Biol.* **1983**, *163*, 119–128.
(21) Duddll, D. A.; Morris, R. J.; Richard, J. T. *Biochim. Biophys. Acta* **1980**, *621*, 1–8.
(22) Findsen, W.; Ondrias, M. R. *Photochem. Photobiol.* **1990**, *51*, 741–748.
(23) Friedman, J. M.; Lyons, K. B. *Nature* **1980**, *284*, 570–572.
(24) Martin, J. L.; Mignus, A.; Poyart, C.; Lecarpentier, Y.; Astier, R., Antonetti, A. *Proc. Natl. Acad. Sci. U.S.A.* **1983**, *80*, 173–177.
(25) Noble, R. W.; Brunori, M.; Wyman, J.; Antonini, E. *Biochemistry* **1967**, *6*, 1216–1222.
(26) Cassoly, R.; Gibson, Q. H. *J. Mol. Biol.* **1975**, *91*, 301–313.
(27) Hoffman, B. M.; Gibson, Q. H. *Proc. Natl. Acad. Sci. U.S.A.* **1978**, *75*, 21–25.
(28) Noble, R. W.; Brunori, M.; Wyman, J.; Antonini, E. *Biochemistry* **1967**, *6*, 1216–1222.
(29) Gibson, Q. H.; Ainworth, S. *Nature* **1957**, *180*, 1416–1417.
(30) Petrich, J. W.; Lambry, J.-C.; Kuczera, K.; Karplus, M.; Poyart, C.; Martin, J.-L. *Biochemistry* **1991**, *30*, 3975–3987.
(31) Hoshino, M.; Kogure, M. *J. Phys. Chem.* **1989**, *93*, 5478–5484.
(32) Hoshino, M.; Ueda, K.; Takahashi, M.; Yamaji, M.; Hama, Y.; Miyazaki, Y. *J. Phys. Chem.* **1992**, *96*, 8863–8870.
(33) Traylor, T. G.; Luo, J.; Simon, J. A.; Ford, P. C. *J. Am. Chem. Soc.* **1992**, *114*, 4340–4345.
(34) Traylor, T. G.; Magde, D.; Luo, J.; Walda, K. N.; Bandyopadhyay, D.; Wu, G.-Z.; Sharma, V. S. *J. Am. Chem. Soc.* **1992**, *114*, 9011–9017.

0002-7863/93/1515-9568$04.00/0 

detailed studies have not yet been made for the nitric oxide adducts of ferrihemoproteins.

The present paper reports absorption spectroscopic studies on equilibrium formation of the nitrosyl adducts of iron(III) porphyrins, (NO)$Fe^{III}$P, and laser flash photolysis studies of (NO)-$Fe^{III}$P. The porphyrin complexes studied here are a water-soluble iron(III) porphyrin, $[Fe^{III}(H_2O)(TPPS)]^{3-}$ ($H_2TPPS^{4-}$ = tetra-anionic form of *meso*-tetrakis(*p*-sulfonatophenyl)porphyrin), and the ferric forms of hemoglobin, myoglobin, cytochrome *c*, and catalase. The photochemistry of several nitric oxide adducts of the ferrous forms, $[Fe^{II}(TPPS)]^{4-}$ and hemoproteins, have also been studied for comparison with that of ferric forms.

## Experimental Section

Water-soluble iron porphyrin, $[Fe^{III}(H_2O)(TPPS)]^{3-}$, was synthesized from the reaction of $(Na)_4(H_2TPPS)$ and iron(III) sulfate in water and purified by cation exchange columns according to the literature.[38] Oxidized forms of hemoglobin (human), myoglobin (whale skeletal muscle), and cytochrome *c* (horse heart) and $(Na)_4(H_2TPPS)$ supplied by Sigma were used without further purification. Catalase from bovine liver with the activity 4000 units/mg was supplied by Wako Pure Chemical Ind. Ltd. Distilled water (pH 6.5) was used as a solvent. The aqueous solutions were not buffered in order to avoid the effects of ions on the photochemical reactions of the nitrosyl complexes.

Optical absorption spectra were recorded on a Hitachi 330 spectrophotometer. Laser photolysis studies were carried out with second (532 nm), third (355 nm), and fourth (266 nm) harmonics and a Nd:YAG laser (HY 500 from JK Lasers, Ltd.): the duration of a laser pulse is ca. 20 ns, and the energies of laser pulses are 200, 100, and 70 mJ per pulse at 532, 355, and 266 nm, respectively. The detection system of transient spectra has been reported elsewhere.[39]

All samples were prepared with the use of a vacuum line to avoid contamination by oxygen: aqueous solutions of hemoproteins were degassed on the vacuum line without freezing the solutions to avoid denaturing of the proteins, and nitric oxide gas was introduced into the solution after degassing. The concentrations of NO in solutions were calculated from the partial pressure of NO gas and a Bunsen absorption coefficient of NO ($4.21 \times 10^{-2}$ at 1 atm and 293 K). The pressures of the nitric oxide gas were measured by a mercury manometer.

## Results

**Absorption Spectroscopic Studies. (1) $Fe^{III}$TPPS and $Fe^{II}$-TPPS.** The absorption spectrum of $Fe^{III}$TPPS in an aqueous solution exhibits peaks at 393 and 528 nm with the molar absorption coefficients $1.55 \times 10^5$ and $1.22 \times 10^4$ $M^{-1}$ $cm^{-1}$, respectively. Figure 1 shows the absorption spectral changes observed for an aqueous solution of $1.0 \times 10^{-5}$ M $Fe^{III}$TPPS at various NO concentrations. The spectral change is reversible. With changing [NO], the spectra display isosbestic points, indicating that the equilibrium is simply expressed as

$$Fe^{III}TPPS + NO \underset{k_d(Fe^{III})}{\overset{k_f(Fe^{III})[NO]}{\rightleftarrows}} (NO)Fe^{III}TPPS \qquad (1)$$

The equilibrium constant, *K*, was determined from the spectral changes. With the use of the molar absorption coefficients ($\epsilon_{Fe}$ and $\epsilon_{NO}$) and the concentrations ($C_{Fe}$ and $C_{NO}$) of $Fe^{III}$TPPS and

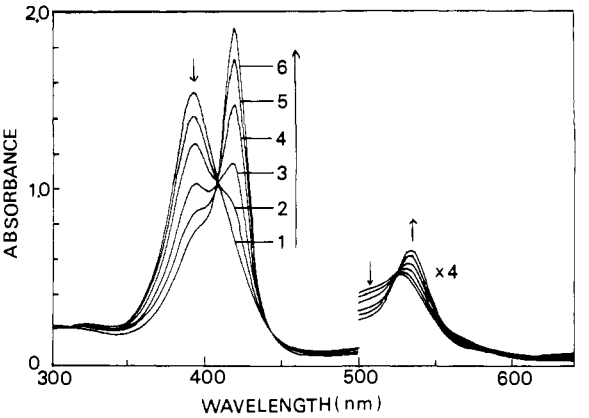


**Figure 1.** Absorption spectral changes of $1.0 \times 10^{-5}$ M $Fe^{III}$TPPS in an aqueous solution in the presence of NO: 1, [NO] = 0 M; 2, [NO] = $1.06 \times 10^{-4}$ M; 3, [NO] = $2.43 \times 10^{-4}$ M; 4, [NO] = $6.0 \times 10^{-4}$ M; 5, [NO] = $1.15 \times 10^{-3}$ M; 6, [NO] = $1.43 \times 10^{-3}$ M.

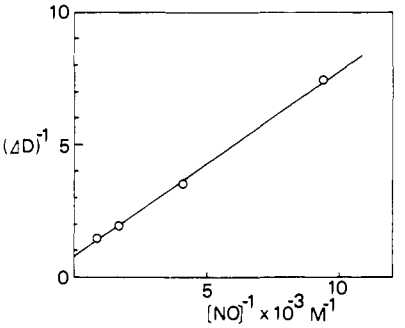


**Figure 2.** Plot of $(\Delta D)^{-1}$ at 393 nm vs $[NO]^{-1}$ for determination of the equilibrium constant for $Fe^{III}$TPPS + NO $\rightleftarrows$ (NO)$Fe^{III}$TPPS.

(NO)$Fe^{III}$TPPS, the absorbance *D* at a wavelength λ is given by

$$D = \epsilon_{Fe}C_{Fe} + \epsilon_{NO}C_{NO} \qquad (2)$$

Since

$$K(Fe^{III}) = k_f(Fe^{III})/k_d(Fe^{III}) = C_{NO}/C_{Fe}[NO] \qquad (3)$$

eq 2 is transformed to

$$D = D_0 + (\epsilon_{NO} - \epsilon_{Fe})C_0K(Fe^{III})[NO]/(1 + K(Fe^{III})[NO]) \qquad (4)$$

where $C_0 = C_{Fe} + C_{NO}$ and $D_0$ is the initial absorbance of $Fe^{III}$-TPPS at λ in the absence of NO. Equation 4 is further transformed to

$$(\Delta D)^{-1} = (D - D_0)^{-1} = \gamma^{-1} + (\gamma K(Fe^{III}))^{-1}[NO]^{-1} \qquad (5)$$

Here $\gamma = (\epsilon_{NO} - \epsilon_{Fe})C_0$.

Figure 2 shows the plot of $(\Delta D)^{-1}$ at 393 nm vs $[NO]^{-1}$. The plot gives a straight line. The slope and the intercept of the line give the values of $\gamma^{-1}$ and $(\gamma K(Fe^{III}))^{-1}$. From these values, the equilibrium constant $K(Fe^{III})$ is determined as $K(Fe^{III}) = 1.1 \times 10^3$ $M^{-1}$. The absorption spectrum of (NO)$Fe^{III}$TPPS displays peaks at 420 and 533 nm. The molar absorption coefficient, $\epsilon_{NO}$, of (NO)$Fe^{III}$TPP at 420 nm was obtained as $2.56 \times 10^5$ $M^{-1}$ $cm^{-1}$.

An aqueous solution of $Fe^{II}$TPPS was prepared by chemical reduction of $Fe^{III}$TPPS with $Na_2S_2O_4$. The spectrum of $Fe^{II}$-TPPS has absorption peaks at 425 and 555 nm with molar absorption coefficients $2.83 \times 10^5$ and $1.12 \times 10^4$ $M^{-1}$ $cm^{-1}$, respectively. When the solution was exposed to NO gas, (NO)$Fe^{II}$-TPPS was produced.

$$Fe^{II}TPPS + NO \xrightarrow{k_f(Fe^{II})[NO]} (NO)Fe^{II}TPPS \qquad (6)$$

The reaction proved to be irreversible, and the resulting spectrum

(35) Traylor, T. G.; Magde, D.; Taube, D. J.; Jongeward, K. A.; Bandyopadhyay, D.; Luo, J.; Walda, K. N. *J. Am. Chem. Soc.* **1992**, *114*, 417–429.
(36) Muray, L. P.; Hofrichter, J.; Henry, E. R.; Ideda-Saito, M.; Kiagishi, K.; Yonetani, T.; Eaton, W. A. *Proc. Natl. Acad. Sci. U.S.A.* **1988**, *85*, 2151–2155.
(37) Hofrichter, J.; Henry, E. R.; Sommer, J. H.; Deutsch, R.; Ikeda-Saito, M.; Kitagishi, K.; Yonetani, T.; Eaton, W. A. *Biochemistry* **1985**, *24*, 2667–2679.
(38) Barley, M. H.; Takeuchi, K. J.; Meyer, T. J. *J. Am. Chem. Soc.* **1986**, *108*, 5876–5885.
(39) Hoshino, M.; Imamura, M.; Watanabe, S.; Hama, Y. *J. Phys. Chem.* **1984**, *88*, 45–49.

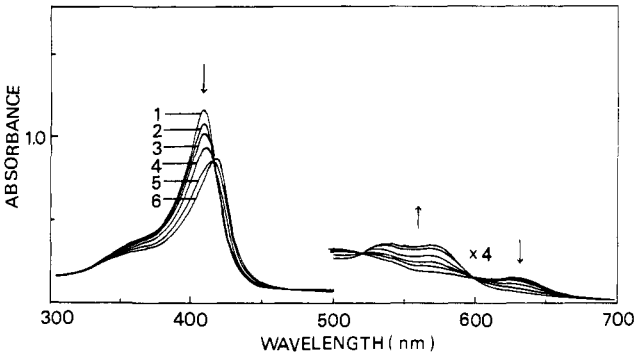


**Figure 3.** Absorption spectral changes of $7.8 \times 10^{-6}$ M $Mb^{III}$ in an aqueous solution in the presence of NO: 1, [NO] = 0 M; 2, [NO] = $1.52 \times 10^{-5}$ M; 3, [NO] = $4.3 \times 10^{-5}$ M; 4, [NO] = $1.44 \times 10^{-4}$ M; 5, [NO] = $3.34 \times 10^{-4}$ M; 6, [NO] = $9.44 \times 10^{-4}$ M.

of $(NO)Fe^{II}TPPS$ displayed peaks at 412 and 542 nm with molar absorption coefficients $1.55 \times 10^5$ and $9.56 \times 10^3$ $M^{-1}$ $cm^{-1}$, respectively.

**(2) Methemoglobin and Hemoglobin.** The spectrum of methemoglobin, $Hem^{III}$, has an absorption peak at 403 nm, while that of hemoglobin, $Hem^{II}$, has peaks at 428 and 553 nm. When the aqueous solution of $Hem^{III}$ was exposed to NO gas (250 Torr), new bands appeared at 417 nm in the Soret band region and 532 and 563 nm in the Q band region, owing to the formation of $(NO)Hem^{III}$. After a few minutes, the latter bands were red-shifted to 542 and 570 nm, while that at 417 nm decreased only slightly in intensity. The overall spectral change was interpreted as the reductive nitrosylation of $Hem^{III}$,[3] since the spectrum of $(NO)Hem^{II}$ produced by the reaction of $Hem^{II}$ and NO also has absorption peaks at 417, 542, and 570 nm. Thus, the reaction of $Hem^{III}$ and NO is apparently represented by

$$Hem^{III} + NO \underset{k_d(Hem^{III})}{\overset{k_f(Hem^{III})}{\rightleftarrows}} (NO)Hem^{III} \qquad (7)$$

$$(NO)Hem^{III} \rightarrow (NO)Hem^{II} \qquad (8)$$

Similar reductive nitrosylation has been reported for the reaction of $ClFe^{III}TPP$ (TPP = tetraphenylporphyrin) in ethanol.[40]

**(3) Metmyoglobin and Myoglobin.** The electronic spectrum of metmyoglobin, $Mb^{III}$, in an aqueous solution exhibits absorption maxima at 408 ($\epsilon = 1.5 \times 10^5$ $M^{-1}$ $cm^{-1}$) and 500 nm ($\epsilon = 1.0 \times 10^4$ $M^{-1}$ $cm^{-1}$). Figure 3 shows the reversible spectral changes observed for the aqueous solution of $Mb^{III}$ at various concentrations of NO.

$$Mb^{III} + NO \underset{k_d(Mb^{III})}{\overset{k_f(Mb^{III})[NO]}{\rightleftarrows}} (NO)Mb^{III} \qquad (9)$$

The absorption peaks of $(NO)Mb^{III}$ are located at 418 ($\epsilon = 2.0 \times 10^5$ $M^{-1}$ $cm^{-1}$), 536, and 570 nm. The equilibrium constant, $K(Mb^{III}) = k_f(Mb^{III})/k_d(Mb^{III})$, obtained from the spectral changes is $1.41 \times 10^4$ $M^{-1}$.

The spectrum of myoglobin, $Mb^{II}$, in an aqueous solution has bands at 432 ($\epsilon = 1.16 \times 10^5$ $M^{-1}$ $cm^{-1}$) and 555 nm.[41] The introduction of NO gas into the aqueous solution led to the irreversible formation of $(NO)Mb^{II}$ with absorption maxima at 420 ($\epsilon = 1.29 \times 10^5$ $M^{-1}$ $cm^{-1}$), 545, and 578 nm.

**(4) Oxidized and Reduced Cytochrome *c*.** The absorption spectrum of oxidized cytochrome *c*, $Cyt^{III}$, in an aqueous solution displays peaks at 408 ($\epsilon = 1.0 \times 10^5$ $M^{-1}$ $cm^{-1}$) and 528 nm

(40) Wayland, B. B.; Olson, L. W. *J. Chem. Soc., Chem. Commun.* **1973**, *897–898*.

(41) Antonini, E.; Brunori, M. *Hemoglobin and Myoglobin in Their Reactions with Ligands*; North-Holland: Amsterdam, 1971.

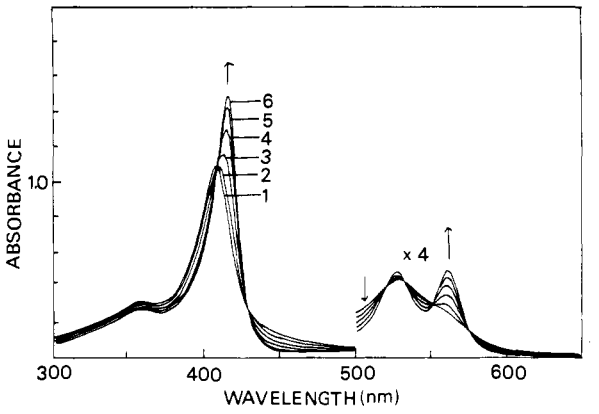


**Figure 4.** Absorption spectral changes of $1.1 \times 10^{-5}$ M $Cyt^{III}$ in an aqueous solution in the presence of NO: 1, [NO] = 0 M; 2, [NO] = $1.01 \times 10^{-5}$ M; 3, [NO] = $3.04 \times 10^{-5}$ M; 4, [NO] = $8.86 \times 10^{-5}$ M; 5, [NO] = $2.56 \times 10^{-4}$ M; 6, [NO] = $1.01 \times 10^{-3}$ M.

($\epsilon = 1.1 \times 10^4$ $M^{-1}$ $cm^{-1}$).[42] Figure 4 shows the absorption spectral changes observed for the aqueous solution of $Cyt^{III}$ after exposure to NO gas. The spectral changes, which exhibit isosbestic points, are interpreted in terms of the reversible formation of the nitric oxide adduct of $Cyt^{III}$, $(NO)Cyt^{III}$.

$$Cyt^{III} + NO \underset{k_d(Cyt^{III})}{\overset{k_f(Cyt^{III})[NO]}{\rightleftarrows}} (NO)Cyt^{III} \qquad (10)$$

The equilibrium constant, $K(Cyt^{III}) = k_f(Cyt^{III})/k_d(Cyt^{III})$, was obtained as $1.63 \times 10^4$ $M^{-1}$. The absorption spectrum of $(NO)Cyt^{III}$ has peaks at 415 ($\epsilon = 1.45 \times 10^5$ $M^{-1}$ $cm^{-1}$), 527 ($\epsilon = 1.0 \times 10^4$ $M^{-1}$ $cm^{-1}$), and 560 nm.

The spectrum of reduced cytochrome, $Cyt^{II}$, in an aqueous solution exhibits absorption peaks at 413, 518, and 549 nm. $Cyt^{II}$ reacts very slowly with NO.

$$Cyt^{II} + NO \xrightarrow{k_f(Cyt^{II})[NO]} (NO)Cyt^{II} \qquad (11)$$

The rate for the formation of the nitric oxide adduct of $Cyt^{II}$ increased with an increase in [NO]. The second-order rate constant, $k_f(Cyt^{II})$, is obtained as 8.3 $M^{-1}$ $s^{-1}$. After 12 h, $Cyt^{II}$ in the aqueous solution, which was exposed to NO gas at 300 Torr, completely changed to $(NO)Cyt^{II}$. It was also found that the rate for the thermal dissociation of NO from $(NO)Cyt^{II}$ was very slow. When the excess NO gas was removed from the solution on the vacuum line, $(NO)Cyt^{II}$ gradually regenerated $Cyt^{II}$ with the first-order rate constant $2.87 \times 10^{-5}$ $s^{-1}$.

$$(NO)Cyt^{II} \xrightarrow{k_d(Cyt^{II})} Cyt^{II} + NO \qquad (12)$$

The equilibrium constant $K(Cyt^{II})$ was determined as $3.0 \times 10^5$ $M^{-1}$ from the ratio of the rate constants $k_f(Cyt^{II})/k_d(Cyt^{II})$.

**(5) Catalase.** Catalase, $Cat^{III}$, is an enzyme which has four protohematin units in a molecule. The absorption spectrum of $Cat^{III}$ in an aqueous solution has absorption peaks at 403 ($\epsilon = 4.3 \times 10^5$ $M^{-1}$ $cm^{-1}$) and 620 nm.[43] As shown in Figure 5, the solution shows the growth of new absorption peaks at 428 ($\epsilon = 4.0 \times 10^5$ $M^{-1}$ $cm^{-1}$), 537, and 574 nm with an increase in the concentration of NO. The spectral changes exhibit isosbestic points. The equilibrium reaction is expressed as shown below.

$$Cat^{III} + NO \underset{k_d(Cat^{III})}{\overset{k_f(Cat^{III})[NO]}{\rightleftarrows}} (NO)Cat^{III} \qquad (13)$$

The equilibrium constant, $K(Cat^{III}) = k_f(Cat^{III})/k_d(Cat^{III})$, obtained as described above from the spectral change is $1.8 \times 10^5$

(42) Margoliash, E.; Frohwirt, N. *Biochem. J.* **1959**, *71*, 570–572.

(43) Fasman, G. D. *Practical Handbook of Biochemistry and Molecular Biology*, CRC Press: Boca Raton, 1989.

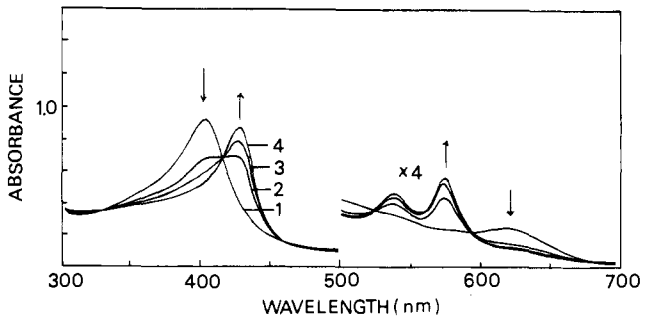


**Figure 5.** Absorption spectral changes of $2.1 \times 10^{-6}$ M $Cat^{III}$ in an aqueous solution in the presence of NO: 1, [NO] = 0 M; 2, [NO] = $1.77 \times 10^{-5}$ M; 3, [NO] = $2.28 \times 10^{-5}$ M; 4, [NO] = $7.57 \times 10^{-4}$ M.

**Table I.** Equilibrium Constants for Association of Axial NO[a]

| reaction | equilibrium constant ($M^{-1}$) |
|---|---|
| $Fe^{III} + NO \rightleftarrows (NO)Fe^{III}TPPS$ | $K(Fe^{III}) = 1.1 \times 10^3$ |
| $Mb^{III} + NO \rightleftarrows (NO)Mb^{III}$ | $K(Mb^{III}) = 1.4 \times 10^4$ |
| $Cyt^{III} + NO \rightleftarrows (NO)Cyt^{III}$ | $K(Cyt^{III}) = 1.6 \times 10^4$ |
| $Cat^{III} + NO \rightleftarrows (NO)Cat^{III}$ | $K(Cat^{III}) = 1.8 \times 10^5$ |
| $Cyt^{II} + NO \rightleftarrows (NO)Cyt^{II}$ | $K(Cyt^{II}) = 2.89 \times 10^5$ |

[a] The equilibrium constants for $Hem^{III}$, $Hem^{II}$, $Mb^{II}$, and $Cat^{II}$ could not be obtained (see text). Experimental errors are ±10%.

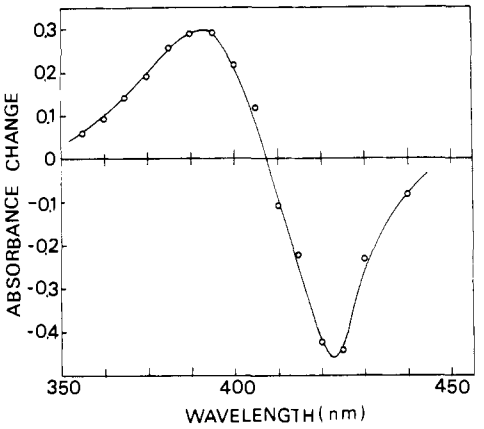


**Figure 6.** Transient absorption spectrum observed for an aqueous solution of $(NO)Fe^{III}TPPS$ in the presence of $1.15 \times 10^{-3}$ M NO, 50 ns after 355-nm laser pulsing.

$M^{-1}$. The chemical reduction of $Cat^{III}$ by $Na_2S_2O_4$ was unsuccessful, so no studies could be done for $Cat^{II}$.

The equilibrium constants, $K$, obtained in the present study are listed in Table I.

**Laser Flash Photolysis Studies. (1) $(NO)Fe^{III}TPPS$ and $(NO)Fe^{II}TPPS$.** Figure 6 shows the transient absorption spectrum observed 50 ns after an aqueous solution of $(NO)Fe^{III}TPPS$ at $1.15 \times 10^{-3}$ M NO was subjected to a laser pulse at 355 nm. The transient is in good agreement with the difference spectrum obtained by subtracting the spectrum of $(NO)Fe^{III}TPPS$ from that of $Fe^{III}TPPS$. The photoreaction, therefore, is expressed as

$$(NO)Fe^{III}TPPS + h\nu \rightarrow Fe^{III}TPPS + NO \qquad (14)$$

The transient spectrum decays uniformly over the whole wavelength range studied according to first-order kinetics with a rate constant of $1.58 \times 10^3$ $s^{-1}$. No permanent photoproduct was detected. These results indicate that the transient $Fe^{III}TPPS$ returns to $(NO)Fe^{III}TPPS$ according to reaction 1. It, therefore, would be expected that the rate constant, $k_1$, for the decay of the transient $Fe^{III}TPPS$ in the presence of excess NO is represented by

$$k_1 = k_f(Fe^{III})[NO] + k_d(Fe^{III}) \qquad (15)$$

Figure 7 shows the straight line plot of the first-order decay rate constant, $k_1$, represented as a function of [NO]. From the slope and the intercept of the line, $k_f$ and $k_d$ are respectively determined as $7.2 \times 10^5$ $M^{-1}$ $s^{-1}$ and $6.8 \times 10^2$ $s^{-1}$. The equilibrium constant, $K(Fe^{III})$, was calculated from the rate constant ratio $k_f(Fe^{III})/k_d(Fe^{III})$ to be $1.06 \times 10^3$ $M^{-1}$, in agreement with that ($1.1 \times 10^3$ $M^{-1}$) obtained from the spectroscopic studies. Photodissociation of NO from $(NO)Fe^{III}TPPS$ was also found to occur upon excitation at 532 nm.

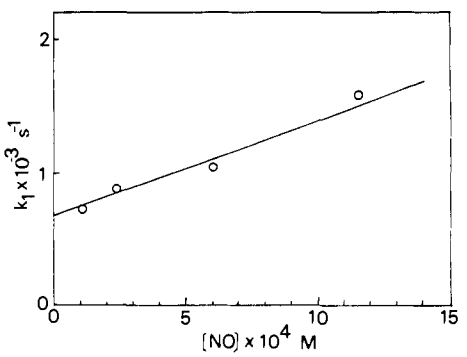


**Figure 7.** Plot of the decay rate constants, $k_1$, for the decay of $Fe^{III}TPPS$ as a function of [NO].

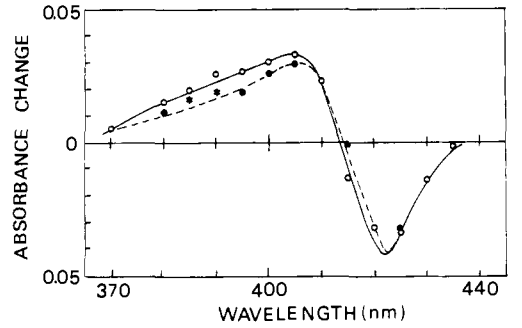


**Figure 8.** Transient absorption spectrum observed for an aqueous solution of $(NO)Mb^{III}$ in the presence of $1.0 \times 10^{-3}$ M NO, 50 ns (○) and 4.5 μs (●) after 355-nm laser pulsing.

As mentioned above, $Fe^{II}TPPS$ irreversibly reacts with NO to yield $(NO)Fe^{II}TPPS$. The laser photolysis studies revealed that $(NO)Fe^{II}TPPS$ photodissociated NO, resulting in the formation of $Fe^{II}TPPS$ according to the difference spectra. The decay of $Fe^{II}TPPS$ follows first-order kinetics in the presence of excess NO to regenerate $(NO)Fe^{II}TPPS$. The plot of the first-order rate constant for the decay of $Fe^{II}TPPS$ vs [NO] is a straight line, and the slope and the intercept give $k_f(Fe^{II}) = 1.8 \times 10^9$ $M^{-1}$ $s^{-1}$ and $k_d(Fe^{II}) < 10^6$ $s^{-1}$, respectively.

**(2) $(NO)Hem^{III}$ and $(NO)Hem^{II}$.** Because $(NO)Hem^{III}$ spontaneously reduces to $(NO)Hem^{II}$, no laser photolysis studies could be made for $(NO)Hem^{III}$. The laser photolysis of an aqueous solution of $(NO)Hem^{II}$ confirmed that only a small amount of $Hem^{II}$ is photochemically produced from $(NO)Hem^{II}$: the yield, Φ, was roughly estimated as $<10^{-3}$ upon excitation at both 355 and 532 nm. Because of the low yield of $Hem^{II}$, the rate constants for association between NO and $Hem^{II}$ and dissociation of NO from $(NO)Hem^{II}$ could not be obtained.

Femtosecond photolysis of $(NO)Hem^{II}$ has shown that the major product is a geminate pair in which NO is trapped at the heme pocket.[18,30] The geminate pair disappears within a few hundred picoseconds by geminate recombination. Since the duration of the laser pulses used in the present study is ca. 20 ns, the transient such as geminate pairs with a lifetime shorter than 20 ns could not be detected. Therefore, the quantum yields reported here are concerned with longer lived species, i.e., those where NO is fully dissociated from the heme.

**(3) $(NO)Mb^{III}$ and $(NO)Mb^{II}$.** Figure 8 shows the transient absorption spectra observed for an aqueous solution of $(NO)Mb^{III}$ plus $1.0 \times 10^{-3}$ M NO for time delays of 50 ns and 4.5 μs after a 355-nm laser pulse. There were modest differences between

these two transient spectra, particularly in the short-wavelength region ($\lambda < 420$ nm). Since the spectrum detected at 4.5 $\mu$s after pulsing closely resembles the difference spectrum ($Mb^{III}$ – (NO)-$Mb^{III}$), one is tempted to suggest that the photoreaction of (NO)-$Mb^{III}$ is represented by the following sequence:

$$(NO)Mb^{III} + h\nu \rightarrow Mb^{III}_{tr} + NO \quad (16)$$

$$Mb^{III}_{tr} \rightarrow Mb^{III} \quad (17)$$

where $Mb^{III}_{tr}$, which is produced from (NO)$Mb^{III}$ immediately after laser pulsing, is assumed to be a species slightly different from $Mb^{III}$, perhaps a different protein conformation. The time-dependent spectral change of the transient observed in the time interval 50 ns-4.5 $\mu$s after pulsing would then be attributed to the conformation change which transforms $Mb^{III}_{tr}$ to $Mb^{III}$. The further slow decay of $Mb^{III}$ to give (NO)$Mb^{III}$ followed first-order kinetics with a rate constant of $k_2 = 2.1 \times 10^2$ s$^{-1}$ at $1.0 \times 10^{-3}$ M NO. The rate constant $k_2$ increases with an increase in the NO concentration:

$$k_2 = k_f(Mb^{III})[NO] + k_d(Mb^{III}) \quad (18)$$

From the plot of $k_2$ vs [NO] the value of $k_f(Mb^{III})$ is obtained as $k_f(Mb^{III}) = 1.9 \times 10^5$ M$^{-1}$. From this value and the equilibrium constant $K(Mb^{III})$ (Table I), $k_d(Mb^{III})$ was calculated to be 13.6 s$^{-1}$.

Laser photolysis of an aqueous solution of (NO)$Mb^{II}$ resulted in the formation of $Mb^{II}$ with a low quantum yield, $\Phi < 10^{-3}$. No determination of the rate constants for association and dissociation of NO could be made.

**(4) (NO)$Cyt^{III}$ and (NO)$Cyt^{II}$.** Figure 9 shows the initial transient absorption spectrum observed for an aqueous solution of (NO)$Cyt^{III}$ in the presence of $1.5 \times 10^{-3}$ M NO 50 ns after a 355-nm laser pulse. This disagrees markedly with the difference spectrum ($Cyt^{III}$–(NO)$Cyt^{III}$), particularly in the short-wavelength region ($\lambda < 405$ nm). By contrast, the transient spectrum recorded 200 $\mu$s after the pulse is in good accord with the difference spectrum ($Cyt^{III}$ – (NO)$Cyt^{III}$). The absorbance changes between the two transient spectra followed first-order kinetics with a rate constant of $(5.5 \pm 0.3) \times 10^3$ s$^{-1}$. Since the rate constant is independent of [NO] in the range $2.1 \times 10^{-4}$–$1.5 \times 10^{-3}$ M, the reaction with free NO cannot be responsible for the spectral change of the transient. Again, one explanation may be that the initial transient is $Cyt^{III}_{tr}$ with a protein conformation different from that of uncomplexed $Cyt^{III}$. According to that model, the photochemistry of (NO)$Cyt^{III}$ would be represented by the sequence of events

$$(NO)Cyt^{III} + h\nu \rightarrow Cyt^{III}_{tr} + NO \quad (19)$$

$$Cyt^{III}_{tr} \rightarrow Cyt^{III} \quad (20)$$

and the time-dependent spectral change of the initial transient would be ascribed to reaction 20. Since no permanent photoproduct is detected for the aqueous solution of (NO)$Cyt^{III}$, $Cyt^{III}$ reacts further with NO to regenerate (NO)$Cyt^{III}$. The decay of $Cyt^{III}$ followed first-order kinetics with the rate constant 1.12 s$^{-1}$ at $1.5 \times 10^{-3}$ M NO.

According to reaction 10, the rate constant, $k_3$, for the decay of $Cyt^{III}$ is formulated as

$$k_3 = k_f(Cyt^{III})[NO] + k_d(Cyt^{III}) \quad (21)$$

From the plot of $k_3$ vs [NO], $k_f(Cyt^{III})$ is obtained as $7.2 \times 10^2$ M$^{-1}$ s$^{-1}$. With the use of the $k_f(Cyt^{III})$ value and the equilibrium constant $K(Cyt^{III})$ (Table I), $k_d(Cyt^{III})$ was calculated to be 4.4 $\times 10^{-2}$ s$^{-1}$.

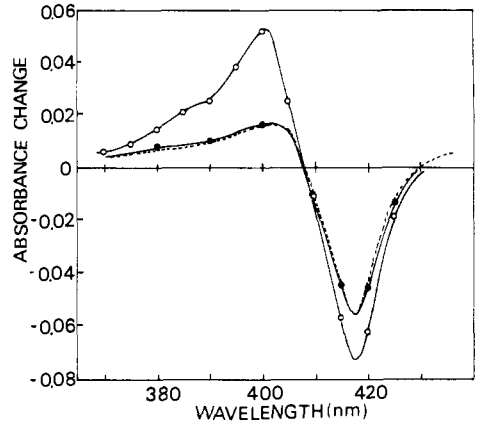


**Figure 9.** Transient absorption spectra observed for an aqueous solution of (NO)$Cyt^{III}$ in the presence of $1.5 \times 10^{-3}$ M NO, 50 ns (○) and 200 $\mu$s (●) after 355-nm laser pulsing. The difference spectrum (- - -) obtained by subtracting the spectrum of (NO)$Cyt^{III}$ from that of $Cyt^{III}$ is also shown for comparison.

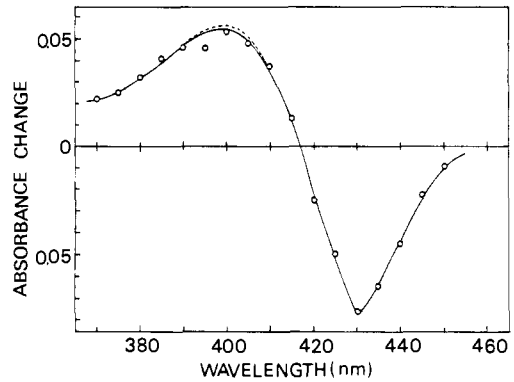


**Figure 10.** Transient absorption spectrum observed for an aqueous solution of (NO)$Cat^{III}$ in the presence of $7.6 \times 10^{-4}$ M NO, 50 ns (○) after 355-nm laser pulsing. The difference spectrum (- - -) obtained by subtracting the spectrum of (NO)$Cat^{III}$ from that of $Cat^{III}$ is shown for comparison.

Laser photolysis studies have confirmed that photodissociation of NO hardly occurs from (NO)$Cyt^{II}$ upon laser excitation at both 355 and 532 nm.

**(5) (NO)$Cat^{III}$.** Figure 10 shows the transient absorption spectrum observed for an aqueous solution of (NO)$Cat^{III}$ plus $7.6 \times 10^{-4}$ M NO 50 ns after a 355-nm laser pulse. This spectrum is in good agreement with the difference spectrum ($Cat^{III}$ – (NO)-$Cat^{III}$), indicating that (NO)$Cat^{III}$ photodissociates NO to give $Cat^{III}$.

$$(NO)Cat^{III} + h\nu \rightarrow Cat^{III} + NO \quad (22)$$

The transient spectrum decays uniformly in the wavelength region studied according to first-order kinetics in the presence of excess NO. No permanent photoproduct was detected after laser photolysis of (NO)$Cat^{III}$. The transient species $Cat^{III}$ is, therefore, considered to react with NO, resulting in the regeneration of (NO)$Cat^{III}$. According to the equilibrium reaction 13, the decay rate constant, $k_4$, is expressed as

$$k_4 = k_f(Cat^{III})[NO] + k_d(Cat^{III}) \quad (23)$$

Figure 11 shows the plot of $k_4$ as a function of the concentration of NO. The plot gives a straight line. From the slope, $k_f(Cat^{III})$ was determined to be $3.0 \times 10^7$ M$^{-1}$ s$^{-1}$. However, the intercept of the line was too small for $k_d$ to be determined precisely. Indeed, the equilibrium constant, $K(Cat^{III})$ (Table I), and forward rate constant, $k_f(Cat^{III})$, were used to calculate $k_d(Cat^{III}) = 1.7 \times 10^2$ s$^{-1}$.

In Table II are listed the rate constants, $k_f$ and $k_d$, for the formation and dissociation of the nitric oxide adducts.

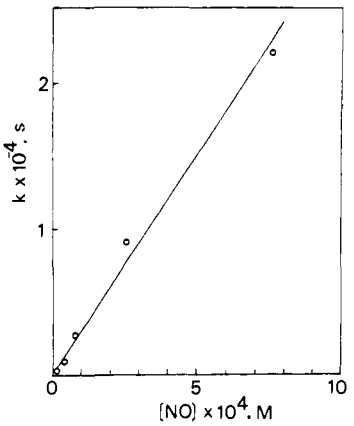


**Figure 11.** Plot of the decay rate constants, $k_4$, for the decay of $Cat^{III}$ as a function of [NO].

**Table II.** Rate Constants for Association and Dissociation of Axial NO[a]

| reaction | rate constant ($k_f$, $M^{-1}$ $s^{-1}$; $k_d$, $s^{-1}$) |
|---|---|
| $Fe^{III}TPPS + NO \rightarrow (NO)Fe^{III}TPPS$ | $k_f(Fe^{III}) = 7.2 \times 10^5$ |
| $Mb^{III} + NO \rightarrow (NO)Mb^{III}$ | $k_f(Mb^{III}) = 1.9 \times 10^5$ |
| $Cyt^{III} + NO \rightarrow (NO)Cyt^{III}$ | $k_f(Cyt^{III}) = 7.2 \times 10^2$ |
| $Cat^{III} + NO \rightarrow (NO)Cat^{III}$ | $k_f(Cat^{III}) = 3.0 \times 10^7$ |
| $Fe^{II}TPPS + NO \rightarrow (NO)Fe^{II}TPPS$ | $k_f(Fe^{II}) = 1.8 \times 10^9$ |
| $Hem^{II} + NO \rightarrow (NO)Hem^{II}$ | $k_f(Hem^{II}) = 2.5 \times 10^7$ [b] |
| $Mb^{II} + NO \rightarrow (NO)Mb^{II}$ | $k_f(Mb^{II}) = 1.7 \times 10^7$ [b] |
| $Cyt^{II} + NO \rightarrow (NO)Cyt^{II}$ | $k_f(Cyt^{II}) = 8.3$ |
| $(NO)Fe^{III}TPPS \rightarrow Fe^{III}TPPS + NO$ | $k_d(Fe^{III}) = 6.8 \times 10^2$ |
| $(NO)Mb^{III} \rightarrow Mb^{III} + NO$ | $k_d(Mb^{III}) = 13.6$ |
| $(NO)Cyt^{III} \rightarrow Cyt^{III} + NO$ | $k_d(Cyt^{III}) = 4.4 \times 10^{-2}$ |
| $(NO)Cat^{III} \rightarrow Cat^{III} + NO$ | $k_d(Cat^{III}) = 1.7 \times 10^2$ |
| $(NO)Fe^{II}TPPS \rightarrow Fe^{II}TPPS + NO$ | $k_d(Fe^{II}) \sim 0$ |
| $(NO)Hem\text{-}\alpha^{II}$ [c] $\rightarrow Hem\text{-}\alpha^{II} + NO$ | $k_d(Hem\text{-}\alpha^{II}) = 4.6 \times 10^{-5}$ [b] |
| $(NO)Mb^{II} \rightarrow Mb^{II} + NO$ | $k_d(Mb^{II}) = 1.2 \times 10^{-4}$ [b] |
| $(NO)Cyt^{II} \rightarrow Cyt^{II} + NO$ | $k_d(Cyt^{II}) = 2.87 \times 10^{-5}$ |

[a] The rate constants for $Hem^{III}$, $Hem^{II}$, $Mb^{II}$, and $Cat^{II}$ could not be obtained (see text). Experimental errors are ±10%. [b] Reference 50. [c] α-Chain of hemoglobin subunit.

**Quantum Yield Measurements for Photodissociation of NO.** Quantum yields for photodissociation of NO adducts were measured with the use of the laser photolysis method.[44,45] When the photoreaction is expressed as

$$(NO)FeP + h\nu \rightarrow FeP + NO \qquad (24)$$

the yield, $\Phi_{dis}$, is formulated as

$$\Phi_{dis} = \Delta OD_i/[\Delta\epsilon d Q_{abs}(D,\lambda)V^{-1}] \qquad (25)$$

where $\Delta OD_i$ is the initial absorbance change observed after laser pulsing, $\Delta\epsilon$ is the difference in the molar absorption coefficient between FeP and (NO)FeP, $D$ is the absorbance of (NO)FeP at the laser wavelength, $d$ is the optical path length of observation, $V$ is the volume of the solution irradiated by the laser pulse, and $Q_{abs}(D,\lambda)$ is the number of quanta absorbed by (NO)FeP. The actinometric method of determining the $Q_{abs}(D,\lambda)$ was to measure quantitatively the triplet–triplet absorption of $^3[Zn^{II}TPP]^*$ (TPP = tetraphenylporphyrin) in a benzene solution having the same absorbance $D$ at the laser excitation wavelength. With the use of the molar absorption coefficient, $\epsilon_T$, of the triplet $Zn^{II}TPP$ at 470 nm and the triplet yield, $\Phi_{ST}$, $Q_{abs}(D,\lambda)$ is expressed as

$$Q_{abs}(D,\lambda) = OD_T/(\epsilon_T d V^{-1}\Phi_{ST}) \qquad (26)$$

where $OD_T$ is the initial absorbance of $^3[Zn^{II}TPP]^*$ at 470 nm observed after laser pulsing and $V$, $d$, and $Q_{abs}$ are the same for the two types of experiments. Substitution of eq 26 into eq 25 gives

$$\Phi_{dis} = (\Delta OD_i\epsilon_T\Phi_{ST})/(\Delta\epsilon OD_T) \qquad (27)$$

Since (1) $\epsilon_T$ and $\Phi_{ST}$ are $7.3 \times 10^4$ $M^{-1}$ $cm^{-1}$ and 0.83, respectively,[46] and (2) $\Delta\epsilon$ is obtained from the difference spectrum (FeP – (NO)FeP), the quantum yield $\Phi_{dis}$ can be readily calculated by eq 27.

**Table III.** Quantum Yields for Full Photodissociation of NO[a] from Nitric Oxide Adducts in Aqueous Solution upon Excitation at 355 and 532 nm

| NO adducts | $\Phi_{dis}$ (355 nm) | $\Phi_{dis}$ (532 nm) |
|---|---|---|
| $(NO)Fe^{III}TPPS$ | 0.37 ± 0.03 | 0.34 ± 0.03 |
| $(NO)Mb^{III}$ | 0.027 ± 0.003 | 0.036 ± 0.004 |
| $(NO)Cyt^{III}$ | 0.034 ± 0.003 | 0.056 ± 0.005 |
| $(NO)Cat^{III}$ | 0.050 ± 0.005 | 0.056 ± 0.005 |
| $(NO)Fe^{II}TPPS$ | 0.16 ± 0.02 | 0.16 ± 0.02 |
| $(NO)Hem^{II}$ | ~0 | ~0 |
| $(NO)Mb^{II}$ | $\leq 10^{-3}$ | $\leq 10^{-3}$ |
| $(NO)Cyt^{II}$ | $\leq 10^{-3}$ | $\leq 10^{-3}$ |

[a] The quantum yields for $(NO)Hem^{III}$ and $(NO)Cat^{II}$ could not be obtained (see text). The yields of geminate pairs, in which NO is trapped at the heme pocket, could not be measured because of the long duration (20 ns) of the laser pulse.

The quantum yield for photodissociation of NO from (NO)-$Fe^{III}TPPS$ in the aqueous solution was determined to be 0.37 upon laser excitation at 355 nm. Excitation at 532 nm gave the yield 0.34; thus, there was no excitation wavelength dependence. The iron(II) analog $(NO)Fe^{II}TPPS$ photodissociates NO with the quantum yield 0.16 upon laser excitation at both 355 and 532 nm.

For $(NO)Hem^{III}$, the quantum yield for photodissociation of NO cannot be measured because of the fast thermal conversion to $(NO)Hem^{II}$. The yield for photodissociation of NO from (NO)-$Hem^{II}$ proved to be smaller than $10^{-3}$.

As stated above, $(NO)Mb^{III}$ photodissociates NO to yield $Mb^{III}_{tr}$ as an initial product which changes to $Mb^{III}$. The yield for the formation of $Mb^{III}$ was determined to be 0.027 and 0.036 upon laser excitation at 355 and 532 nm, respectively. In contrast, the quantum yield for photodissociation of NO from $(NO)Mb^{II}$ was estimated to be below $10^{-3}$.

Laser photolysis studies also demonstrated that photodenitrosylation of $(NO)Cyt^{III}$ initially gives $Cyt^{III}_{tr}$, which thermally relaxes to $Cyt^{III}$. The overall yields for the formation of $Cyt^{III}$ from $(NO)Cyt^{III}$ were found to be 0.034 and 0.056 upon excitation at 355 and 532 nm, respectively. Only a small amount of $Cyt^{II}$ was found to be produced photochemically from $(NO)Cyt^{II}$: the yield is as low as $10^{-3}$.

Laser photolysis of $(NO)Cat^{III}$ generates $Cat^{III}$ with the quantum yields 0.05 and 0.056 upon laser excitation at 355 and 532 nm, respectively.

In Table III are listed the quantum yields for the photodissociation of NO from the nitric oxide adducts studied.

## Discussion

Physical and chemical properties of hemoproteins are markedly affected by the nature of proteins surrounding the heme. Therefore, the photochemical properties of the protein-free complexes, $(NO)Fe^{III}TPPS$ and $(NO)Fe^{II}TPPS$, were investigated for the appropriate comparisons.

The absorption spectrum of $Fe^{III}TPPS$ in an aqueous solution exhibits a peak maximum at 393 nm in the Soret band region. The peak is red-shifted from 393 to 420 nm by forming the nitric oxide adduct, $(NO)Fe^{III}TPPS$. This result has been interpreted

(44) Hoshino, M.; Kogure, M.; Amano, K.; Hinohara, T. *J. Phys. Chem.* **1989**, *93*, 6655–6659.
(45) Hoshino, M.; Kashiwagi, Y. *J. Phys. Chem.* **1990**, *94*, 673–678.
(46) Hurley, J. K.; Sinai, N.; Linschitz, H. *Photochem. Photobiol.* **1983**, *38*, 9–14.

in terms of a charge-transfer interaction from NO to the metal center such as $(NO^+)Fe^{II}TPPS$.[1,2] On the other hand, the absorption peak of $Fe^{II}TPPS$ at 425 nm is blue-shifted to 412 nm by forming $(NO)Fe^{II}TPPS$. Analogous shifts of Soret bands were observed for the ferric and ferrous hemoproteins on exposure to NO. The Soret bands of ferric forms shift toward red, but those of the ferrous forms shift toward blue.

The equilibrium constants for association of NO are in the order $Cat^{III}$ ($1.8 \times 10^5$ $M^{-1}$) > $Cyt^{III}$ ($1.6 \times 10^4$ $M^{-1}$) ~ $Mb^{III}$ ($1.4 \times 10^4$ $M^{-1}$) > $Fe^{III}TPPS$ ($1.1 \times 10^3$ $M^{-1}$). The fact that the equilibrium constants of $Cat^{III}$, $Mb^{III}$, and $Cyt^{III}$ are an order of magnitude larger than that of $Fe^{III}TPPS$ suggests that the surrounding proteins regulate the rates for both association and dissociation processes of NO from the heme.

Photodissociation of NO from $(NO)Fe^{III}TPPS$ gives a transient spectrum identical with the difference spectrum ($Fe^{III}TPPS$–$(NO)Fe^{III}TPPS$), indicating the photochemical formation of $Fe^{III}$-TPPS. No change in the transient spectrum is observed during the course of the decay. Similar observations were made for $(NO)Fe^{II}TPPS$ and $(NO)Cat^{III}$.

In contrast, laser photolysis of $(NO)Mb^{III}$ affords $Mb^{III}_{tr}$ as an initial transient which relaxes to $Mb^{III}$. The spectrum of $Mb^{III}_{tr}$ resembles but is different from that of $Mb^{III}$.[47] According to the crystal structures of $Mb^{III}$, the fifth and sixth axial positions of the heme in $Mb^{III}$ are occupied by imidazole moieties of both distal and proximal histidine residues. The central iron(III) atom in $Mb^{III}$ is considered to interact with the remote imidazole of the distal histidine more weakly than with the close one. When the imidazole moiety of the histidine residue is replaced by NO, there would be a resulting change in the protein conformation of $Mb^{III}$ to minimize the strain. The initial product, $Mb^{III}_{tr}$, from the photolysis of $(NO)Mb^{III}$ may be assumed to have a protein conformation similar to that of $(NO)Mb^{III}$. The resulting strained $Mb^{III}_{tr}$ undergoes relaxation within a few microseconds to give $Mb^{III}$. The Soret absorption band of $Mb^{III}_{tr}$ is slightly blue-shifted in comparison with that of $Mb^{III}$. The similar conformation change in the protein of $Mb^{II}$ has been suggested on the basis of the laser photolysis studies of the dioxygen adduct of $Mb^{II}$.[48]

According to the X-ray structure, the fifth and sixth axial positions of the central iron(III) atom in $Cyt^{III}$ are occupied by a histidine imidazole moiety and a methionine sulfur, respectively.[49] When NO reacts with $Cyt^{III}$, it replaces an axial ligand, presumably the methionine sulfur, which is a weaker ligand than imidazole. Thus, the conformation of the protein in $(NO)Cyt^{III}$ should differ from that in $Cyt^{III}$. The initial transient spectrum observed for $(NO)Cyt^{III}$ 50 ns after laser pulsing was different from the ($Cyt^{III}$ – $(NO)Cyt^{III}$) difference spectrum, particularly in the short-wavelength region ($\lambda < 405$ nm). This observation can be interpreted in terms of the protein conformations: laser photolysis of $(NO)Cyt^{III}$ would yield, as the initial product, $Cyt^{III}_{tr}$ with a protein structure close to that of $(NO)Cyt^{III}$. Recoordination of the axial methionine sulfur may require changes in the protein conformation, and the relatively slower relaxation of the spectrum of $Cyt^{III}_{tr}$ to that of $Cyt^{III}$ may reflect this process. Transformation of $Cyt^{III}_{tr}$ to $Cyt^{III}$ takes place with the first-order rate constant $5.5 \times 10^3$ $s^{-1}$.

Since the sixth axial ligand of $Cyt^{III}$, methionine S, is tightly bound to the central iron atom, the protein conformational changes incurred by $Cyt^{III}$ upon nitrosylation may be much larger than those by $Mb^{III}$. If, as mentioned above, the protein conformations of $Cyt^{III}_{tr}$ and $Mb^{III}_{tr}$ are close to those of their respective nitrosyl analogs, the conformational differences between $Cyt^{III}_{tr}$ and $Cyt^{III}$ are likely to be larger than those between $Mb^{III}_{tr}$ and $Mb^{III}$. This proposal is supported by the finding that the rate for $Cyt^{III}_{tr} \rightarrow Cyt^{III}$ transformation is slower than that for $Mb^{III}_{tr} \rightarrow Mb^{III}$. Furthermore, the spectral differences between $Mb^{III}_{tr}$ and $Mb^{III}$ are much less than those between $Cyt^{III}_{tr}$ and $Cyt^{III}$. However, the latter observation must be quantified by noting that the studies here are limited by the time window for detection (ca. 50 ns). Thus, spectral changes may be influenced by differing rates and efficiencies of geminate pair recombination for the various systems, processes which require picosecond or femtosecond detection methods to be explored in detail.[14,18,51]

The rate constants for the relaxations of $Cyt^{III}_{tr} \rightarrow Cyt^{III}$ and $Mb^{III}_{tr} \rightarrow Mb^{III}$ do not depend on [NO] below ca. $1 \times 10^{-3}$ M. This indicates that the rate for the reaction between $Cyt^{III}_{tr}$ and free NO is slower than that for the relaxation of $Cyt^{III}_{tr}$ to $Cyt^{III}$.

The transient spectrum observed for $(NO)Cat^{III}$ after laser pulsing is almost identical with the difference spectrum ($Cat^{III}$ – $(NO)Cat^{III}$). This observation suggests that differences in the protein structure between $(NO)Cat^{III}$ and $Cat^{III}$ are very small. Since $Cat^{III}$ is an enzyme which catalyzes the thermal decomposition of $H_2O_2$ into $O_2$ and $H_2O$, the sixth axial position, which is free from a ligand, is expected to be exposed to the water phase in order to allow the access of $H_2O_2$. Nitrosylation of $Cat^{III}$, therefore, should readily occur at the sixth axial position without significant protein structure changes.

The rate constants, $k_f$, for the nitrosylation follow the order $Cat^{III}$ ($3.0 \times 10^7$ $M^{-1}$ $s^{-1}$) ≫ $Fe^{III}TPPS$ ($7.2 \times 10^5$ $M^{-1}$ $s^{-1}$) > $Mb^{III}$ ($1.9 \times 10^5$ $M^{-1}$ $s^{-1}$) ≫ $Cyt^{III}$ ($7.2 \times 10^2$ $s^{-1}$). $Cyt^{III}$ gives the smallest rate constant for nitrosylation, probably due to the occupation of the sixth axial position by a sulfur atom in the methionine moiety. It is noteworthy that $k_f(Cat^{III})$ is ca. 40 times larger than $k_f(Fe^{III})$. In constrast to the cases of $Mb^{III}$ and $Cyt^{III}$, where the protein retards nitrosylation rates, the rate for nitrosylation of $Cat^{III}$ is strongly accelerated by the protein in $Cat^{III}$.

The rate constants for denitrosylations follow the order $(NO)Fe^{III}TPPS$ ($6.8 \times 10^2$ $s^{-1}$) > $(NO)Cat^{III}$ ($1.7 \times 10^2$ $s^{-1}$) > $(NO)Mb^{III}$ ($1.36 \times 10$ $s^{-1}$) > $(NO)Cyt^{III}$ ($4.4 \times 10^{-2}$ $s^{-1}$). In each case, the ferrihemoproteins release NO with a rate constant smaller than that of $(NO)Fe^{III}TPPS$, suggesting that the proteins retard the denitrosylation process.

The laser photolysis studies demonstrate that $(NO)Fe^{II}TPPS$ efficiently photodissociates to give $Fe^{II}TPPS$. The rate constant for nitrosylation, $k_f(Fe^{II})$, is determined to be $1.8 \times 10^9$ $M^{-1}$ $s^{-1}$, reasonably close to the rate constant, $5.2 \times 10^9$ $M^{-1}$ $s^{-1}$, for bimolecular reaction between NO and $Fe^{II}TPP$ in benzene.[31] The value of $k_f(Fe^{II})$ was found to be $2.5 \times 10^3$ times larger than $k_f(Fe^{III})$, and the equilibrium constants must be much larger for NO adduct formation. These results indicate that the binding energy between NO and $Fe^{II}$ in $Fe^{II}TPPS$ must be stronger than that between NO and $Fe^{III}$ in $Fe^{III}TPPS$. Similarly, the equilibrium constant for formation of $(NO)Cyt^{II}$ is larger than that for formation of the $(NO)Cyt^{III}$ analog (Table I).

Yields for photodissociation of NO from $(NO)Hem^{II}$, $(NO)$-$Mb^{II}$, and $(NO)Cyt^{II}$ are so small ($\Phi < 10^{-3}$) that the present nanosecond laser photolysis method could not be used for the measurements of the rate constants for the association of NO with $Hem^{II}$, $Mb^{II}$, and $Cyt^{II}$. However, the rate constants, $k_f$-($Cyt^{II}$) and $k_d(Cyt^{II})$, could be obtained with the measurement of the time-dependent absorption spectral changes of $Cyt^{II}$ in the presence of NO and of $(NO)Cyt^{II}$ in the absence of NO, respectively. As shown in Table II, it is found that $k_f(Cyt^{II}) \ll k_f(Cyt^{III})$. This result is very contrary to the cases of $Fe^{II}TPPS$ and $Mb^{II}$, $k_f(Fe^{II}) \gg k_f(Fe^{III})$ and $k_f(Mb^{II}) \gg k_f(Mb^{III})$, and suggests that the sixth ligand in $Cyt^{II}$ is more strongly bound to the central iron atom than that in $Cyt^{III}$.

(47) Mattews, B. W. In *The Proteins*; Neurath, H, Hill, R. L., Boeder, C.-L., Eds.; Academic Press: New York, 1977; Vol. III, Chapter 4.
(48) Satoh, F.; Shiro, Y.; Sakaguchi, Y.; Suzuki, T.; Iizuka, T.; Hayashi, H. *J. Biol. Chem.* **1990**, *265*, 2004–2010.
(49) Dickerson, R. E.; Takano, T.; Eisenberg, T.; Kallai, O. B.; Cooper, A.; Margoliash, E. *J. Biol. Chem.* **1971**, *246*, 1511.
(50) Moore, E. G.; Gibson, Q. H. *J. Biol. Chem.* **1976**, *251*, 2788–2794.
(51) Petrich, J. W.; Martin, J. L.; Houde, D.; Poyart, C.; Orszag, A. *Biochemistry* **1987**, *26*, 7914–7923.

The quantum yield, $\Phi_{dis}$, for the photodissociation of NO from (NO)$Fe^{III}$TPPS is obtained as 0.37. As listed in Table III, this value is an order of magnitude larger than those of (NO)$Mb^{III}$, (NO)$Cyt^{III}$, and (NO)$Cat^{III}$, indicating that the effects of the proteins surrounding the heme reduce the quantum yield. The decrease in $\Phi_{dis}$ caused by surrounding proteins is also observed for (NO)$Mb^{II}$ and (NO)$Cyt^{II}$: the yields for photodissociation of NO from (NO)$Mb^{II}$ and (NO)$Cyt^{II}$ are 2 orders of magnitude less than that from (NO)$Fe^{II}$TPPS.

Recent studies[18,30] of nitric oxide adducts of hemoglobin by femtosecond and picosecond laser photolysis have shown that (1) NO is photodissociated from (NO)$Hem^{II}$ within less than 50 fs in the heme pocket and (2) ca. 99% of the NO produced undergoes geminate recombination with $Hem^{II}$ to regenerate (NO)$Hem^{II}$ in the heme pocket within a few hundred picoseconds. Less than 1% NO escapes the heme pocket. Such results indicate that the geminate pair of $Hem^{II}$ and NO would not be detected by the nanosecond laser photolysis system. The present nanosecond laser photolysis study confirmed that the yields for NO photodissociation from the nitric oxide adducts of both oxidized and reduced hemoproteins are very small in comparison with the yields obtained with (NO)$Fe^{III}$TTPS and (NO)$Fe^{II}$TPPS. It is likely that most of the NO photodissociated from the nitric oxide adducts of ferric and ferrous hemoproteins is trapped in the heme pocket and undergoes geminate recombination, leading to small quantum yields for full photodissociation of NO.

Studies of the pH effects on nitrosylferrihemoproteins in buffered aqueous solutions are in progress.

**Acknowledgment.** This work was supported by a grant on Solar Energy Conversion by Means of Photosynthesis from the Science and Technology Agency of Japan. P.C.F. acknowledges a grant from the U.S. National Science Foundation (CHE-9024845) and from the U.S.–Japan Cooperation Research (Photoconversion/Photosynthesis) Program (NSF INT 9116346).